

A Photodiode in Space

Robert Isaksson

Swedish Institute of Space Physics
Uppsala

7th November 2005

Contents

1	Introduction	1
1.1	Cassini's journey	1
1.2	Purpose	1
2	The basic physics	3
2.1	The photoelectric effect	3
2.2	Plasma - the medium of space	3
3	The Sun, the Earth, Saturn	5
3.1	The Sun and the solar spectrum	5
3.2	The Earth and E10.7, a measure of UV-intensity at the Earth . . .	6
3.3	Saturn and its moons	6
3.4	The Sun, observed from the Earth and Saturn	7
3.5	Solar data, observed from the Earth and Saturn	7
4	The environment in space	9
4.1	The solar wind - the space between the planets	9
4.2	The bow chock	10
4.3	The magnetosheath - a turbulent region	10
4.4	The magnetopause	10
4.5	The magnetosphere - inside the planets magnetic field	10
4.6	The ionosphere- the end of space and the beginning of the atmosphere	11
5	The satellites	13
5.1	Cassini and Huygens	14
5.2	Cassini Orbiting Saturn	14
5.3	Pioneer Venus Orbiter (PVO)	15

6	How to measure EUV and photoemission	17
6.1	The Langmuir probe	17
6.2	How to measure EUV	17
6.3	Output data	19
6.4	The physical problem to be solved	20
7	Calibration model	21
7.1	Choice of Calibration Method	21
7.2	Analytical Method	21
7.3	Experimental Method	22
7.4	Statistical Method	22
8	Method	23
8.1	Selection of Calibration Data	23
8.2	Selection of Reference Data	24
8.3	Equation to Solve	24
8.4	Method to Solve the Equation	25
8.5	Assumptions	26
8.5.1	Results from PVO	26
8.5.2	Other assumptions	26
8.6	Data selection criteria	26
8.6.1	Data Selection E10.7 - The Earth and Saturn	26
8.6.2	Cassini	26
8.6.3	The Langmuir probe - the potential sweep	27
8.7	Limitation	27
9	Evaluating the method	29
9.1	Evaluation Criteria	29
9.2	Test of the Method	29
9.3	The three tests in detail	29
9.4	Test 1	29
9.4.1	Description	29
9.4.2	Aim	30
9.4.3	Data selection	30
9.4.4	Expected result	30
9.5	Test 2	30
9.5.1	Description	30
9.5.2	Aim	30
9.5.3	Data selection	31
9.5.4	Expected result	31

9.6	Test 3	31
9.6.1	Description	31
9.6.2	Aim	31
9.6.3	Data selection	32
9.6.4	Expected results	32
10	Implementation	33
10.1	Data administration	33
10.1.1	Cassini - the potential sweep	33
10.1.2	Data selection	33
10.1.3	E10.7	33
10.1.4	Calculating the calibration value	33
10.1.5	Estimate the UV-intensity	34
10.1.6	Selecting the I-data	34
11	Data quality analysis	35
11.1	Solar wind	35
11.2	Inside the magnetopause	36
11.3	Close flybys and the perigee of Saturn	37
11.4	The bias jump	39
11.5	The channels that measure the photocurrent	40
11.6	Noise reduction	41
11.7	Improvement of signal	43
11.8	Identification of Outliers	44
11.8.1	A global lower and higher cut off value	44
11.8.2	A local cut off value, based on a estimation of a normal distribution	45
11.9	Removal of the square wave	46
11.10	Separating the two signals	47
11.11	Classification criteria for the solar wind	48
11.12	Classification criteria for the magnetopause	49
11.13	Unclassified points	49
11.14	Evaluation of the classifiers	50
11.15	Which separator to use	50
11.16	Selecting a reference signal	51
11.17	Merging the two signals	52
11.18	Algorithm for improving the signal	53

12 Result	55
12.1 Result from test 1	55
12.2 Result from test 2	55
12.3 Results from test 3 - without data adjustment	55
12.4 Results from test 3 - with data adjustment	57
13 Conclusions and Discussion	61
13.1 Conclusion of test results	61
13.2 Conclusion of the data analysis	61
13.3 Discussion about the cause of the square wave	61

List of Figures

3.1	The Sun, Earth and Saturn	5
4.1	The magnetosphere	9
5.1	Cassini at Saturn	13
6.1	The Langmuir probe	18
6.2	A potential sweeps from the Langmuir probe near SOI	19
11.1	Cassini in the solar wind	36
11.2	Histogram of the probe current in the Solar Wind	37
11.3	Histogram E10.7	39
11.4	Cassini in the high density plasma	40
11.5	Histogram of the probe current in high density plasma	41
11.6	The Saturn Flyby at the 29th of October 2004	43
11.7	The mean value and the variance of the potential sweep in the solar wind	44
11.8	The mean value and the variance of the potential sweep in the magnetopause	45
11.9	The distribution of the photocurrent	46
11.10	The distribution of the photocurrent	47
11.11	Data classified in the solar wind	48
11.12	The distribution of the photocurrent	49
11.13	Data classified in the MP	50
11.14	MP data classified with the Solar wind	51
11.15	Solar wind data classified with the MP-classifier	52
12.1	E10.7 and estimated UV-intensity at Venus made by PVO from 1981 to 1984	56

12.2	Estimated UV-intensity in the solar wind at Saturn made by Cassini, without data adjustment	58
12.3	Estimated UV-intensity at Saturn made by Cassini, with signal S_1 and S_2 , 24 hours resolution	59
12.4	Estimated UV-intensity at Saturn made by Cassini, with data adjustment	60

Chapter 1

Introduction

1.1 Cassini's journey

The Cassini spacecraft that carries the moon probe Huygens entered the Saturn system and passed its ring plane during the summer 2004, seven years after it's launch from Earth in 1997. Onboard there is an instrument called a Langmuir probe, which is part of the Radio and Plasma Wave Science (RPWS) investigation [1]. The Cassini/Huygens project is an European-American collaborative project. Following arrival the spacecraft will continue to orbit Saturn for an additional 4-6 years. The Langmuir probe will continuously sample data during this period, which will include close encounters by icy moons and the large intriguing moon of Titan. A Langmuir probe is like a weather station for electrically charged gas, and can give estimates of a number of basic physical parameters such as density and temperature. One important parameter to estimate from the data of the Langmuir probe is the solar UV intensity. It is a vital parameter for some of the instruments on board as it determines the number of photoelectrons around the spacecraft. The UV intensity also determines the degree of solar ionization in the upper atmosphere of Titan and on Saturn. The ionization level in turn affects radio propagation and the possible monitoring of events like lightning in the atmospheres of these bodies.

1.2 Purpose

The aim of this work is to develop a method which uses the Langmuir probe current, caused by the photoelectric effect, to estimate the solar intensity of the sun in the Extreme Ultra Violet spectrum (EUV), in the wavelength range 30 nm to 130 nm.

Chapter 2

The basic physics

2.1 The photoelectric effect

The photoelectric effect was discovered by Albert Einstein and gained him the Nobel Prize in 1921 [2]. The photoelectric effect states that the energy in light is determined by wavelength. When light shines on a metal surface and the incoming light is of high enough energy, i.e. wavelength below a certain threshold, the surface will emit electrons. The number of photons above the threshold in energy and the photoelectric yield of the material determine the numbers of electrons that are emitted. The photoelectric yield is a property of the material that describes the probability for an electron to be emitted at a certain wavelength of the incoming light.

2.2 Plasma - the medium of space

Plasma is a gas made up of free ions and electrons. These free and electrical charged particles are created by EUV-radiation or cosmic rays. The EUV radiation is emitted from the Sun and cosmic rays are charged particles (e^- , p^+ , ions) of high energy in the magnetosphere. Due to the low density there is little chance of collision that would result in that these particles bond to create neutral atoms. Even in the event of a collision the charged particles could easily remain separated because the large temperature and low density in the plasma. The temperature in the plasma is described by the average kinetic energy of the particles.

Chapter 3

The Sun, the Earth, Saturn

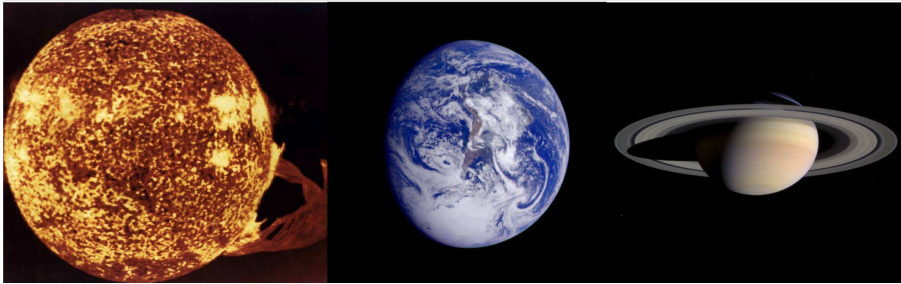


Figure 3.1: The Sun, Earth and Saturn

3.1 The Sun and the solar spectrum

The sun is a body with a rotation period of approximately 27 days as seen from Earth. Because the sun rotates in the same direction as the Earth the sun's rotation will appear slightly faster when it is observed from planets further out in the system compared to the rotation observed at Earth. The solar activity determines the frequency of when different phenomena arise and disappear; e.g. sunspots and solar flares. When these phenomena occur they move around on the surface until they finally disappear. This turns the solar disc into a dynamic disc and the solar activity determines how often these active areas are created and their lifespan. The solar activity follows an 11-year cycle and during the active part of the cycle the frequency of arising solar flares, sunspots and solar storms is higher compared to the passive part of the solar cycle. This changes the solar spectrum of the sun. The

distribution of energy over wavelength changes with the activity of the sun. The section of the sun's light spectrum ranges from hard X-rays with a wavelength of less than 1nm all the way up to far infrared light with a wavelength greater than 40 000 nm. For the purpose of this study the light in the EUV-spectrum, from 30 nm to 130 nm, will be focussed upon. At the end of the EUV-spectrum there is a strong emission line at 121.6 nm, Lyman - α . This emission line arises from the nuclear processes which occur continuously in the sun.

3.2 The Earth and E10.7, a measure of UV-intensity at the Earth

At the Earth we notice when solar activity is high; causing considerable northern light and at worst in the damaging of satellites orbiting earth, the telephone system and power distribution. For this reason the activity of the sun is monitored. E10.7 [3] is a UV-index of the energy/photon distribution over the wavelength, from 1nm to 1 million nm. The E10.7 index is determined by using an empirical solar irradiance model; Solar2000 [3]. The data for this model is collected from a number of satellites orbiting in space around the Earth. The E10.7 index is developed by Space Environment Technologies [4] and the data provided a daily value of photons per second and per cm^2 at 1 AU, which is the average distance from Earth to the sun.

3.3 Saturn and its moons

It takes Saturn 30 years to circle the sun. Therefore, compared to the orbit time for the earth to orbit around the sun and the sun's rotation time, Saturn is practically standing still. Saturn is orbiting at a distance of 9.5 AU from the Sun. Saturn, like the earth, has its own magnetic fields. This magnetic field keeps the atmosphere from being eroded down by the solar wind. Therefore the magnetic field is essential for any planet that has its own atmosphere. Several of Saturn's moons, among those Titan, are orbiting within this magnetic field. Cassini will measure the UV-intensity at Saturn making it possible to measure how its atmosphere is affected by solar light. Cassini will orbit Saturn and pass within close range of Saturn and several of Saturn's moons.

3.4 The Sun, observed from the Earth and Saturn

Even though the Sun has a rotation time of 27-days, Saturn and Earth will not see the same solar disc more than approximately once a year. This will only occur when both planets line up and view the same solar disc. The reason for this is the dynamic surface of the sun, caused by several processes with a short lifespan from a few minutes, e.g. solar flares, to a several years, e.g. the solar cycle . These processes change the surface of the sun as times goes by. Because Saturn's orbit is 30 times longer than that of the Earth there will be approximately 1 year and 11 days between each time they will coincide to line up against the Sun. The first time Saturn and Earth were aligned with the sun after Cassinis arrival to Saturn was in the middle of January 2005. The next time will be at the end of January 2006.

3.5 Solar data, observed from the Earth and Saturn

The correlation in time between solar data from Earth and Saturn depends on the size of the common solar disc that is seen from both planets. When observations are made of the sun from both these planets, they will differ and yet still be correct. The reason for this is the fact that a different part of the sun may have been observed. The correlation between the two observations depends on how large the common solar disc has been. The strongest correlation in time will occur when both planets are aligned with the sun and the weakest will occur when Saturn and the Earth are on opposite side of the sun. *The effect of the changing correlation in time requires caution when comparing the two sets of data, because there is no guarantee that they will show the same event.* This varying time correlation has three different causes. The first is the time difference for the sunrays to hit the planets. It takes 8 minutes from the sun to the earth and 76 minutes from the sun to Saturn. The second cause is the angle between Earth and Saturn as seen from the Sun and the number of days it takes for the Sun to rotate until the same point on the solar disc is visible at respective planet. The third cause is the changing appearance of the surface, with the rise, fall and moving of local structures during the rotation of the sun. Despite the fact that there is a changing correlation in time, it is still possible to compare the two datasets from an average point of view.

Chapter 4

The environment in space

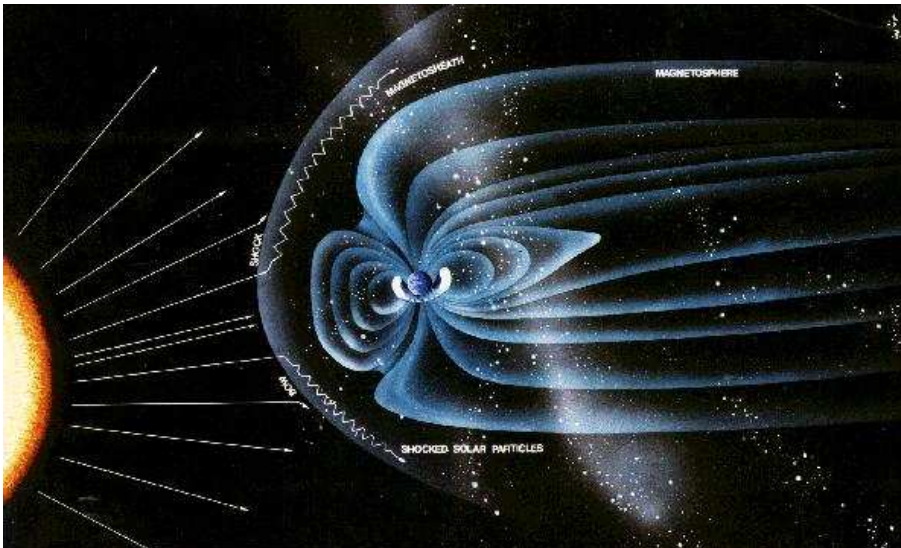


Figure 4.1: The magnetosphere

4.1 The solar wind - the space between the planets

The empty space between the planets does not consist of a vacuum, but it consists of plasma, an electrically charged gas, which travels at a supersonic speed and has its origin in the hot solar corona. This is low-density plasma that radiates away

from the Sun and carries the solar magnetic field. This flow of plasma outwards from the Sun is the solar wind. When the solar wind reaches a planet with a magnetic field, a bow shock is formed. For the purposes of this work, the properties of the solar wind of most interest are that of density and pressure. The solar wind has a low density that makes it possible to measure solar EUV-intensity with with a Langmuir probe. The pressure of the solar wind as it interacts with the planet's internal magnetic field determines the position of the magnetosphere and its sub structures. Inside this boundary the low-density property of the plasma can no longer be guaranteed.

4.2 The bow chock

This is the point at which the solar wind meets the magnetic field of a planet. The speed of the plasma changes, from being supersonic to being subsonic. Fig. 4.1 shows a picture of the bow shock, the magnetosheath, the magnetopause and the magnetosphere.

4.3 The magnetosheath - a turbulent region

Inside the bow shock is the magnetosheath, which is an area consisting of turbulent plasma. The turbulence is caused by the fact that the supersonic solar wind hits the bow shock and becomes subsonic. The density of this plasma is still low, but nevertheless remains higher than that of the solar wind.

4.4 The magnetopause

The magnetopause is a thin boundary region between the solar wind and the planets magnetic field. The turbulence is lower and the density is higher in the magnetopause compared to the magnetosheath.

4.5 The magnetosphere - inside the planets magnetic field

The magnetosphere is caused by the planet's own magnetic field and arises from the interaction between the magnetic field lines which travel with the solar wind and the magnetic field lines surrounding a planet. The position of the magnetosphere is closely related to the pressure of the solar wind. When the pressure changes the magnetosphere adjusts its position at a speed far greater than the speed at which a satellite travels. As the distance between the planet and the magnetosphere is not

4.6. *THE IONOSPHERE- THE END OF SPACE AND THE BEGINNING OF THE ATMOSPHERE* 11

fixed, an estimated distance is often used. Only a planet with an internal magnetic field has a magnetosphere. The magnetospheres of Saturn and Earth are structurally similar. However, Venus has no magnetosphere at all. A magnetosphere looks like a drop of water, the head always pointing toward the sun with the tail orientating in the opposite direction. The density through the magnetosphere changes, from being at the same magnitude as the density of solar wind in the outer region, to much more dense close to the ionosphere.

4.6 The ionosphere- the end of space and the beginning of the atmosphere

Close to the planet is the ionosphere, the top layer of the atmosphere. This is where space ends and the atmosphere begins. The ionosphere is made of plasma. The neutral atmosphere is ionized by the EUV-radiation from the Sun and particle radiation from space. The plasma density increases to a level much higher than the magnetosphere. The EUV-radiation from the sun is a fundamental facilitator in this action. These two processes in the ionosphere split molecules and create a plasma, which initiates a chain of chemical reactions down through the atmosphere.

Chapter 5

The satellites

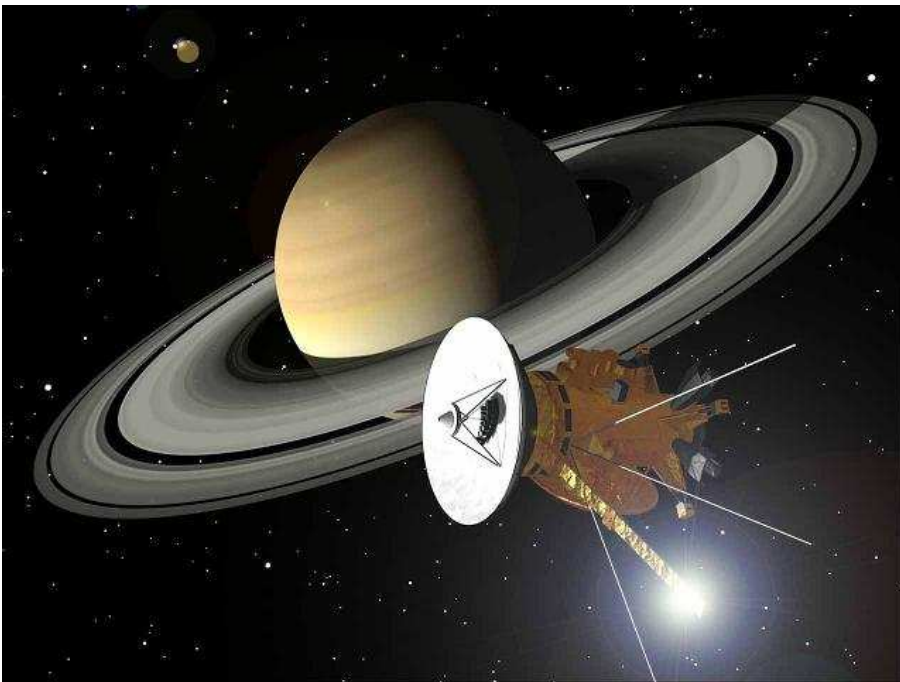


Figure 5.1: Cassini at Saturn

5.1 Cassini and Huygens

In November 1997 the Cassini spacecraft that carries the moon probe Huygens were launched from the Earth, which marked the beginning their seven years long voyage. During the summer of 2004, the satellite reached Saturn and began to orbit the planet. During a close fly-by of the intriguing moon Titan the moon probe Huygens was detached from Cassini. With the aid of a parachute, Huygens successfully landed on the moon's surface in January 2005. Cassini will orbit around Saturn for 4-6 years and during this time it will make several close flybys of Saturn's moons including Titan. During this period in orbit Cassini will continuously send data from the 12 instruments. The Langmuir probe may be used to determine the intensity of EUV-spectrum of the sunlight. This measurement is important for two principal reasons. Firstly, the cloud of electrons that are created by the UV-radiation affect some of the other instruments onboard the satellite. Secondly, the EUV-light is important for the creation of the ionosphere, the top ionized layer of the atmosphere. This plasma layer around the moon affects radio propagation by creating a barrier that blocks the "visibility" of the processes taking place further down in the atmosphere, e.g. detection of events such as lightning. The processes in the ionosphere, caused by the EUV-radiation, occur so rapidly that it is not accurate enough to only use measurements from the Earth as a reference point.

5.2 Cassini Orbiting Saturn

Cassini entered Saturn Orbit Injection (SOI) on the 29th of June 2004 and proceeded to orbit the planet. The subsequent orbits were longer before the satellite's orbit period time stabilized at 15 days. The interesting point concerning the orbit is the length of time the satellite spends in the solar wind where there is low-density plasma. The position of Saturn's magnetopause is estimated to $25 R_S$ [5]. It is not necessary to use a more accurate measurement for the magnetopause as it varies with the solar wind pressure at a speed much higher than the satellite's. However it is important to at least have a rough estimation of where the magnetopause may be. The quality of the measurement of the photocurrent is superior in the solar wind because of the low density of the plasma. Inside the magnetopause the density will begin to increase and at some stage this will begin to affect the data provided by the Langmuir probe. During an orbit Cassini spends most of its time outside the magnetosphere, in the solar wind, and only inside the magnetosphere for a few days. Table 5.1 [6] shows Cassini's orbit pattern beginning with the SOI.

Table 5.1: Cassini's orbit pattern around Saturn

Date of perigee	Orbit length in days	Length of apogee, mAU	Days within $25 R_S$
1/7 -04	120	60	30/6 - 4/7
28/10 -04	48	30	26/10 - 31/10
15/12 -04	32	24	13/12 - 18/12
16/1 -05	32	24	14/1 - 19/1
17/2 -05	20	15	15/2 - 20/2
9/3 -05	21	15	7/3 - 12/3

5.3 Pioneer Venus Orbiter (PVO)

The Pioneer Venus Orbiter (PVO) orbited Venus from 1979 to 1986 and measured the solar EUV-intensity with a cylindrical Langmuir probe [7]. The analytical studies made by this Langmuir probe system forms the theoretical basis to this report. The distance from Venus to the Sun is 0.7 AU. Venus has no magnetic field and therefore has no magnetosphere, but there is an ionosphere. The main results to be considered are the following:

- The photoelectric yield for any metal will roughly be the same.
- Changes within the solar spectrum between solar maximum and solar minimum will have a very small impact on the difference in photoelectric current. This implies that equation (6.1) only need to be solved for one solar spectrum.
- Most photoemission is caused by photons from the EUV-range, less than 3 percent arises from wavelength greater than Lyman- α , 121.6 nm, and the contribution from wavelengths smaller than 50 nm is negligible.
- The total EUV flux is linearly related to the photocurrent.

The most significant differences between the Pioneer and the Cassini project is that Venus has no magnetic field of its own, so there are only disturbances from high-density plasma within the ionosphere. The PVO spacecraft was equipped with two cylindrical Langmuir probes as compared to Cassini's one spherical probe. The probes on PVO were also made of the metals molybdenum and rhenium, while the Langmuir probe on Cassini is made of titanium, with a titanium nitride surface coating.

The photocurrent data from the PVO spacecraft will be used to test the method described in this report.

Chapter 6

How to measure EUV and photoemission

6.1 The Langmuir probe

The Langmuir [8] probe is a part of the Radio and Plasma Wave Science (RPWS) experiment, whose main area of interest is the thin plasma surrounding Saturn and the upper layer of the atmosphere of Titan. A Langmuir probe may be looked upon as a weather station for electrically charged gas, and is able to give estimates of a number of basic physical parameters as density and temperature of the plasma. Another important parameter possible to estimate from the Langmuir probe data, is the solar EUV intensity. Due to the surrounding plasma and the photoelectric effect, a Debye shield of electrical charged particles will form around the spacecraft. In order to measure the plasma accurately the probe should be outside this Debye layer. To accommodate this requirement, the Langmuir probe is placed on a boom. To examine the plasma a sweep is made for different potentials from 32 V to -32 V, relative to the spacecraft. Such a sweep is made most often every 10 minutes as the satellite collects its data. For the positive potentials, electrons in the plasma are attracted and for negative potentials, ions are attracted.

6.2 How to measure EUV

When the probe is illuminated by the EUV-light it starts to emit photoelectrons. This continuous electron emission is a result of the photoelectric effect. The size of the photocurrent depends on two elements: The spectrum of the incoming light and the photoelectric yield of the sunlit surface. The spectrum shows the distribution of photons due to wavelength and intensity and the photoelectric yield shows

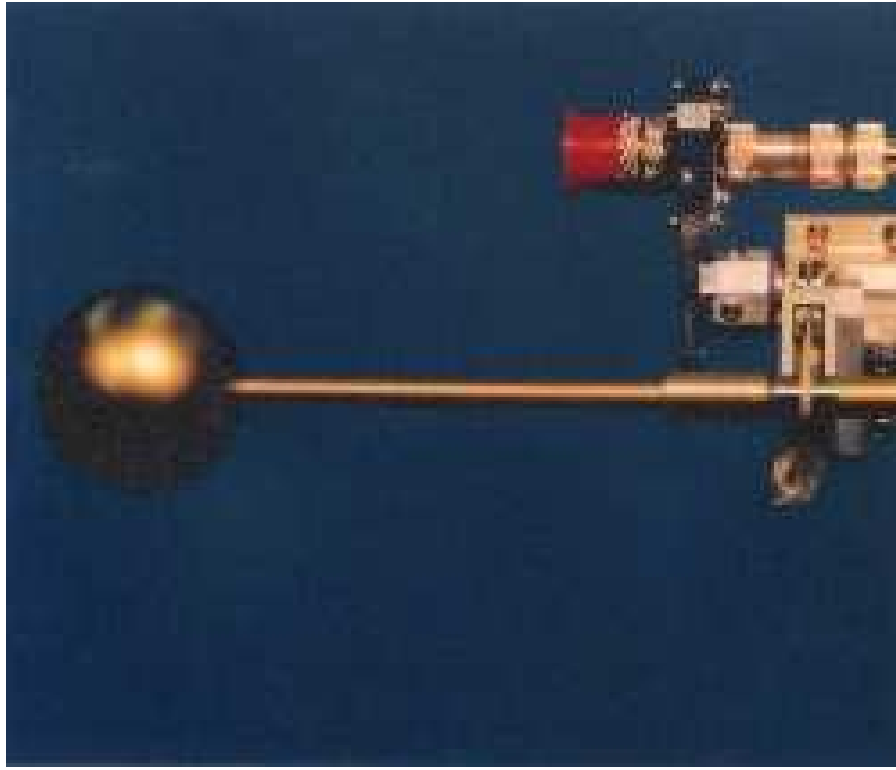


Figure 6.1: The Langmuir probe

the likelihood for a photoelectron emission depending on the wavelength. The equation that connects the photocurrent with the sunlight is [7]:

$$i_{pe} = A_c e \int_0^{\lambda_t} \Phi_\lambda Y_\lambda d\lambda \quad (6.1)$$

This equation shows that most of the photocurrent is caused by radiation from the EUV-range, with a linear relation [7] between the number of photons and the size of the current. The measurement needs to be in the negative part of the potential sweep, so that all the emitted photoelectrons are repelled away from the probe. When measuring the probe current in this range two different currents will be measured. First the intended photocurrent but also an ion-current will be measured. The ion-current is caused by the attraction from the negatively charged probe on the positively charged ions from the surrounding plasma. For this method to be successful the ion-current needs to be small enough to be neglected, which in turn

demands that the surrounding plasma be sufficiently low in density with the probe potential also sufficiently low, but still negative enough to repel all photo electrons, including those emitted from the spacecraft. The potential range which gives the best measurement of the photocurrent, depends on a trade off between having a high negative potential that repels all the emitted electrons and still low enough negative potentials to keep the contamination from the ion current sufficiently small enough to be neglected.

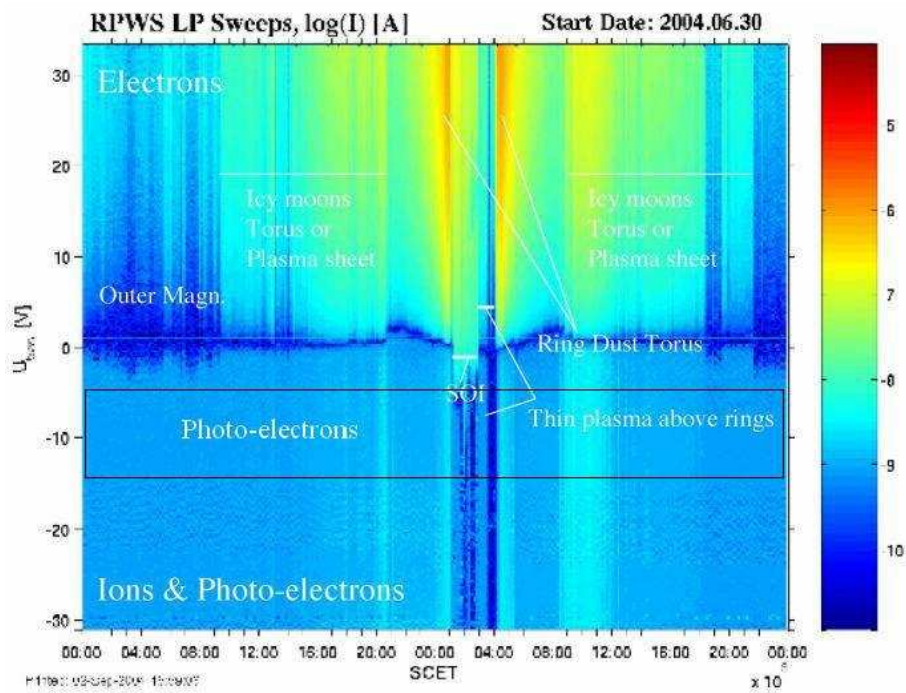


Figure 6.2: A potential sweeps from the Langmuir probe near SOI

6.3 Output data

The Langmuir probe performed a sweep, most of the time, approximately every 10 minutes, from +32 voltages to -32 voltages. Each sweep has 256 point and the unit is in ampere. Figure 6.2 shows a potential sweep from the Langmuir probe.

6.4 The physical problem to be solved

The current measured by the probe:

$$i_{total} = i_{ph} + i_{ion} \quad (6.2)$$

where it is assumed to be

$$i_{ion} \sim 0 \quad (6.3)$$

if the density is low enough. The photocurrent i_{ph} is given by the following equation:

$$i_{ph} = c \int_0^{\lambda_t} \Phi_{\lambda} Y_{\lambda} d\lambda \quad (6.4)$$

where

λ_t - The upper limit of the wavelength of a photon that can create photoelectron emission.

Φ_{λ} - the photoelectric yield as a function of wavelength.

Y_{λ} - the intensity of the solar radiation as a function of wavelength.

Brace et al [7] shows that the total EUV-flux which can be derived from equation (6.4) has a linear relation to i_{ph} .

$$UV_{Venus} = 1.53 \times i_{ph} \quad (6.5)$$

where UV_{Venus} is the total EUV-flux and i_{ph} is in units of 10^{-9} amperes.

Chapter 7

Calibration model

When the satellite was launched from Earth, the Langmuir probe was not calibrated to convert the photocurrent to an UV-intensity. There are three basic approaches that may be employed in order to make this calibration, where all have their advantages and disadvantages. The different calibration methods are as follows: analytical, experimental and statistical.

7.1 Choice of Calibration Method

The choice of an analytical, experimental or statistical solution is not a selection made on the basis of one method being correct whilst the other two are false. The selection is rather based on an assessment of the relevant advantages and disadvantages each method carries, as each method works in a fundamentally different way. The result would not likely be identical if all three methods were implemented. When a selection is made there would need to be a distinction between which method the confidence lies within. This is not to say that the result for the three methods would be widely disparate, on the contrary they would be expected to be closely related.

7.2 Analytical Method

The analytical approach is to solve (6.1) analytically, by knowing the solar spectrum and the photoelectric property of the material. The advantage of this method is that it is easy to solve for several different solar spectra and many different materials. The main disadvantage is that the properties of the probe might change with time and these changes are difficult to predict and compensate for. Changes in the photoelectric yield can be affected by oxidation or absorption particles on

the surface on the probe. This method was used for the Langmuir probe on the PVO spacecraft which orbited around Venus during the years between 1979 and 1986 [7].

7.3 Experimental Method

This method is very straightforward; the photoelectric current is measured in a laboratory. The most significant advantage is relatively clear. This method makes it possible to measure the current without any simplifications, which may lead to errors. The disadvantages are the same as for the analytical model. If the photoelectric yield changes with time, there may be no easy way to compensate for this unknown fluctuation. This method serves as an effective complement to and a reference for other developed methods.

7.4 Statistical Method

The principle of the statistical method is to use the Langmuir probe data of the photoelectric current and correlate those data with the UV-intensity data from the sun. The advantages with this method lie in the fact that several calibrations can be made as the properties of the Langmuir-probe possibly varies with time. The main disadvantage is that this method requires knowledge about the system in order to assume a function which solves the calibration equation. Another problem which may be encountered is if the assumed function not is able to solve the calibration equation, a result is still delivered. For this reason, test data is of vital importance.

Chapter 8

Method

The statistical method has been used to calibrate the Langmuir probe data from Cassini for the following reasons: The satellite will orbit Saturn for several years and produce prolific amounts of data which will make the calibration data sufficiently large. The flybys may change the conditions of the probe's surface and thus it may be necessary to recalibrate. So far, after eight years in space, no changes have been seen. Undertaking the following steps will correlate the Langmuir probe data with the reference data.

1. Assume a function that converts the photocurrent to UV-intensity.
2. Selection of calibration data.
3. Pre-calculation filtering of the data from the Langmuir probe.
4. Compute the current from the Langmuir-probe.
5. Divide the reference data for the UV-intensity into to subsets; a training set (used to set the parameters in the assumed function) and a test set (to evaluate the fitted function).
6. Fit the assumed function in the best possible way to the training data.
7. Evaluate the function against the reference test data.

8.1 Selection of Calibration Data

If the the potential sweep is made in low-density plasma and the probe is sunlit then the current represents all the photons in the EUV-range if the following criteria are fulfilled.

Selection criteria for the calibration data:

- The satellite should be in the solar wind.
- Relevant channels of the potential sweep should be selected.
- Low in noise.

8.2 Selection of Reference Data

E10.7 from Solar 2000 is chosen as reference data. E10.7 provides the intensity of the solar radiation in the solar wind close to Earth for wavelengths from 1 nm to 1 mm. The wavelength resolution for EUV frequencies is 1 nm and the time resolution is per day. Both these resolutions are sufficiently high because the solar variation is a much slower process. The EUV-interval to be examined is from 30 nm to 130 nm and the major part of the photocurrent is caused by photons in the interval 50-125 nm.

8.3 Equation to Solve

The equation (6.4) produces a linear result (6.5) of the UV-intensity at Venus. This makes it possible to assume that a linear equation will solve the relation between the EUV-flux at Saturn and the photocurrent i_{ph} .

$$UV_{Saturn} = c \times i_{ph} + m \quad (8.1)$$

where c and m are the parameters needs to be determined.

By using the fact that no photocurrent will exist if there are no photons in the EUV-range, m may be assumed to be zero.

$$m = 0 \quad (8.2)$$

The reference data is from Earth, at 1 AU, and Saturn is orbiting at 9.5 AU. Geometrical reasons decrease determine the following equation which converts solar intensity from earth to Saturn:

$$UV_{Saturn} = UV_{Earth} / r_{Saturn}^2 \quad (8.3)$$

r_{Saturn} is the average distance between Saturn and the sun, in AU.

By combining the equations (8.1), (8.2) and (8.3) the relation between i_{ph} and the reference data is given:

$$UV_{Earth}/r_{Saturn}^2 = UV_{Saturn} = c \times i_{ph} \quad (8.4)$$

The constant c can be determined by rewriting equation (8.4)

$$c = UV_{Earth}/r_{Saturn}^2/i_{ph} \quad (8.5)$$

8.4 Method to Solve the Equation

The three main differences between the data from Cassini and the data from E10.7 are:

- Weak correlation in time between the Cassini data and E10.7.
- Differences in noise.
- Cassini travels through a changing plasma environment.

The best solution is to choose a two-point fit for the parameter c . One point will be in origin,

$$i_{ph}(zero - photons) = 0 \quad (8.6)$$

The photocurrent from the probe can be defined as:

$$i_{ph} = mean(i_{biaslevel} \in U_{sweep}^{i_{ph}}) \quad (8.7)$$

$U_{sweep}^{i_{ph}}$ are the bias potentials in the sweep that best measures the photocurrent.

The EUV-intensity at Earth can be defined as:

$$UV_{Earth} = mean\left(\sum_{\lambda-min}^{\lambda-max} E10.7\right) \quad (8.8)$$

$\lambda - min$ lower limit of EUV

$\lambda - max$ upper of the EUV-range.

With equation (8.7) and (8.8) the constant c in equation (8.5) is given by the following equation:

$$c = mean(UV_{Saturn})/mean(i_{ph}) = mean\left(\sum_{\lambda-min}^{\lambda-max} \right)/mean(i \in U_{channels}^{i_{ph}}) \quad (8.9)$$

When c is determined the estimation of the UV-intensity can be made by rewriting the equation (8.9) in the following way:

$$UV_{estimation} = c \times mean(i \in U_{channels}^{i_{ph}}) \quad (8.10)$$

8.5 Assumptions

8.5.1 Results from PVO

From the work with the Venus-probe the following assumptions may be made:

- There is a linear relation between the number of photons in the interval 30 nm to 130 nm and the photocurrent from the Langmuir probe.
- The number of photoelectrons caused by photons with wavelength greater than 130 nm is assumed to be zero.
- If the plasma has a sufficiently low density then the current caused by ions may be assumed to be zero.

8.5.2 Other assumptions

- The solar spectrum in the solar wind is assumed to be the same at Saturn as at the Earth.
- The solar disc is assumed to be homogenous after viewing it for a sufficiently long time. This indicates that the average radiation from the Sun is identical from any point in space.

8.6 Data selection criteria

8.6.1 Data Selection E10.7 - The Earth and Saturn

To get the best possible correlation in time between the reference and the satellite data the communal part of the solar disc as seen from both Earth and Saturn need to be as large as possible. The larger the communal solar disc, the better the two datasets will be correlated in time.

8.6.2 Cassini

The Langmuir probe data need to be collected from an environment with low density plasma so the disturbance from surrounding ions becomes as small as possible. For this reason, the best data will be collected in the solar wind. The probe also needs to be sunlit, otherwise the photocurrent will be zero, i.e. not in eclipse by the spacecraft or planetary objects.

8.6.3 The Langmuir probe - the potential sweep

The selected potential intervals for the current-data need to fulfil the following criteria:

- Need to be in the negative part of the sweep to measure the photocurrent.
- Need to be sufficiently negative to repel all the photoelectrons.
- Can not be too negative to avoid a non-negligible ion current.
- Need to be in the range of the potential sweep where the disturbances are as small as possible.

8.7 Limitation

There is no possibility to discover a solar flare with these methods since their life-cycle is often less than 20 minutes and Cassini performs a sweep most often every 10 minutes. This means that the precision of the EUV-intensity decreases during the time periods when the solar intensity is high due to changes in the solar spectrum. These changes are caused by solar flares. The possibility to make a new calibration might increase the precision, but a flare will be difficult to detect and thus can not be removed.

Chapter 9

Evaluating the method

9.1 Evaluation Criteria

Two parameters can be viewed when evaluating the method: The general trend and the bias level of the UV-intensity. These two parameters may be compared with the reference data.

9.2 Test of the Method

Three different tests have been performed to evaluate the method and its functionality. The three tests have three different tasks. The first task is to make sure that the method introduces no false artifacts in the data, the second task is to test the method and the assumptions which the method is based on, and the third task is a test on Cassini.

9.3 The three tests in detail

9.4 Test 1

9.4.1 Description

The calculations in the method may be evaluated using data where the linear relation is known between the input and the output:

$$UV = c_{preassigned} \times mean(I) \quad (9.1)$$

and

$$c_{calibration} = mean(UV)/mean(I) \quad (9.2)$$

If the method is working correctly the calibration result $c_{calibration}$ will be identical to $c_{preassigned}$. The output from the method may also be evaluated from plotted data. Both the bias level and the trends should be identical when the output is compared to the analytically calculated output.

9.4.2 Aim

The aim with this test is to verify that the method gives the result as is equation (9.3), when the the dataset UV is created by a know dataset I and a constant $c_{preassigned}$.

$$c_{calibration} = c_{preassigned} \quad (9.3)$$

9.4.3 Data selection

The dataset I can be a randomly generated dataset.

9.4.4 Expected result

The estimated value of c needs to be identical to the preassigned value of c .

9.5 Test 2

9.5.1 Description

This test will evaluate this statistical method and its assumptions by comparing it against the analytical model used in the PVO. In the PVO-project the calibration was calculated analytically and the result was

$$EUV_{Venus} = 1.53 \times 10^{11} \times i_{prob} \quad (9.4)$$

i_{prob} - in nA

EUV - in photons per second and cm^2

By applying this method to the same data the two solutions can be compared.

9.5.2 Aim

This test will evaluate the method and the assumptions the method is based on. Fundamental assumptions:

- Linear relation between the UV-intensity and the photons in the EUV-range.
- The local variations on the Sun will be negligible after averaging for a sufficient length of time.
- Verify that E10.7 can be used as reference data.

9.5.3 Data selection

The data from the Venus project have been selected from the period between 1981 and 1984 because the satellite experienced problems after June 1985 which rendered the data unreliable. From the PVO there are no strict limits of what is classified as EUV and for that reason the test will be made on the Lyman- α emission line. This emission line is defined as 120 nm to 125 nm and causing 51% of the photocurrent.

9.5.4 Expected result

The previous analytical determined calibration factor and the new calibration factor should be in the same range for the result to be good: $C_{stat} \sim C_{theory}$. As the two planets line up with the sun the difference between bias level in the reference data and the Venus data should decrease, the reference data and the Venus data should show a minimum difference in bias and trend.

9.6 Test 3

9.6.1 Description

One dataset for calibration is selected. By using this calibration the UV-intensity can be estimated for Cassini data. This estimation can be evaluated against the reference data. The following two criteria will be used in the evaluation:

- Are the bias levels of the estimated UV-intensity the same as E10.7.
- Are the same solar trends visible in both datasets.

9.6.2 Aim

The purpose of this test is to determine if the UV-intensity is in the same range as the reference data and to see if trends in the solar data will be visible in both the Cassini and E10.7 sets of data. It is also possible to see when the method fails because of the high density plasma.

9.6.3 Data selection

Optimal data selection would be to take data from several periods when Cassini is in the solar wind and the planets are viewing the same part of the Sun. With this data selection the trends would be easy to identify and the bias levels easy to compare. Because Earth and Saturn only align once since SOI, a longer calibration period of 2-3 solar rotations is necessary to even out local solar variations because of low time correlation. Periods when Cassini is close to Saturn or is doing a flyby of any of the moons will be excluded because the low density plasma can no longer be guaranteed. The data selected for the calibration are from the following dates: 1/6-04 till 20/10-04 with the exception of the period 28/6-04 till 2/7-04 when SOI was performed.

9.6.4 Expected results

A relatively good result should be evident in the periods of time when Cassini is in low density plasma, both from the UV-intensity and the solar trend. It should be possible to see at which distance from Saturn the ion current no longer can be neglected. This can be studied before and after Cassini perigee of Saturn. At this distance the boundary of the method is found because the Langmuir probe is no longer measuring the photo current.

Chapter 10

Implementation

The implementation of this problem contains three different parts: data administration, calibration and UV-estimation

10.1 Data administration

10.1.1 Cassini - the potential sweep

The sweep-data collected from the Langmuir probe is sent to Earth, converted into a current, calibrated and finally stored in the ISDAT-database. From ISDAT it is possible to load the probe data into Matlab-format.

10.1.2 Data selection

Selection from the Langmuir probe data can be made with the following two parameters: a time interval and an interval of the potential levels.

10.1.3 E10.7

The E10.7 data comes in a ASCII-file, created by an external program. The ASCII-file is imported into Matlab, so it is possible to calculate the daily total intensity for the requested time periods and EUV-range.

10.1.4 Calculating the calibration value

Both the Cassini and the E10.7 are average for the corresponding time periods and the calibration value, c , calculated by equation (8.9), is calculated. Due to the weak and variable data correlation no least square linear regression is used. The results in

a calibration-constant which is given in the unit of photons per square centimeters and second. The result is saved in a file together with the input values for the calibration. Two different types of plots are also displayed. The first plot shows the estimated UV-intensity and the E10.7-data for each period. The second plot contains the estimated UV-intensity for all the periods and the E10.7 data. Both of the plots make it possible to visually evaluate the result and and possibly find data that is not likely to be a measure of the photocurrent.

10.1.5 Estimate the UV-intensity

Cassini and E10.7 are loaded as in section 10.1.2 The calibration file is loaded. The estimated UV-intensity is given both as a plot and as an ASCII-file. The estimated UV-intensity is given with a resolution from 1 to 48 hours. The UV-intensity is created by equation (8.10).

10.1.6 Selecting the I-data

All the data within the potential sweep from 0 to -32 volt are assumed to contain the data of the photocurrent and some additional noise above that. Each level of the potential sweep can be viewed as a channel that carries the signal of the Langmuir-probe current. The channels in that range may carry different levels of noise. To exclude potential noisy channels, the mean value and the standard deviation will be measured for each channel. All the channels with widely separated mean-value or higher standard deviations than the rest will not be used in the measurement of the photocurrent.

Chapter 11

Data quality analysis

The data is analysed to determine the quality of the data and to determine if there is some need of filtering it before usage. The data that can be filtered away are outliers or systematic errors. Outliers are data that would not be a measure of the photocurrent, e.g. when Cassini is doing a flyby and travels through high density plasma. Systematically error may be an error in the way of measuring the photocurrent. The basis for the analysis will be a plot of the sweep that the probe does, histogram of selected parts of the signal and the photocurrent as it varies with time. There are three different sections that can be found in the data: When the probe is in the solar wind, within the magnetopause and during close flybys. These three different areas can be identified in the sweep and they all got different characteristics.

11.1 Solar wind

The characteristics that are unique for the solar wind are the very little change in the negative part of the sweep and the alternating values in the positive part of the sweep. This can be seen in the upper plot of figure 11.1. In the photocurrent there is a continuous jump between two levels, (Fig. 11.1 middle plot). When the histogram of the photocurrent is analysed two peaks appear (Fig. 11.1 lower plot). In the histogram over the UV-intensity from E10.7, only one peak is present (Fig. 11.3). When comparing the bias jump of the photocurrent and the changes in the sweep, the conclusion to be made is that they occur at the same time (Fig. 11.1). These plots come from a period of 7 days. When the histogram for the shorter period (Fig. 11.1 lower plot) is compared with the histogram of entire period in the solar wind (Fig. 11.2) the same two peaks occur and the conclusion that can be made is that the bias jump is an ongoing process. Table 11.1 shows the time when

Cassini is in the solar wind.

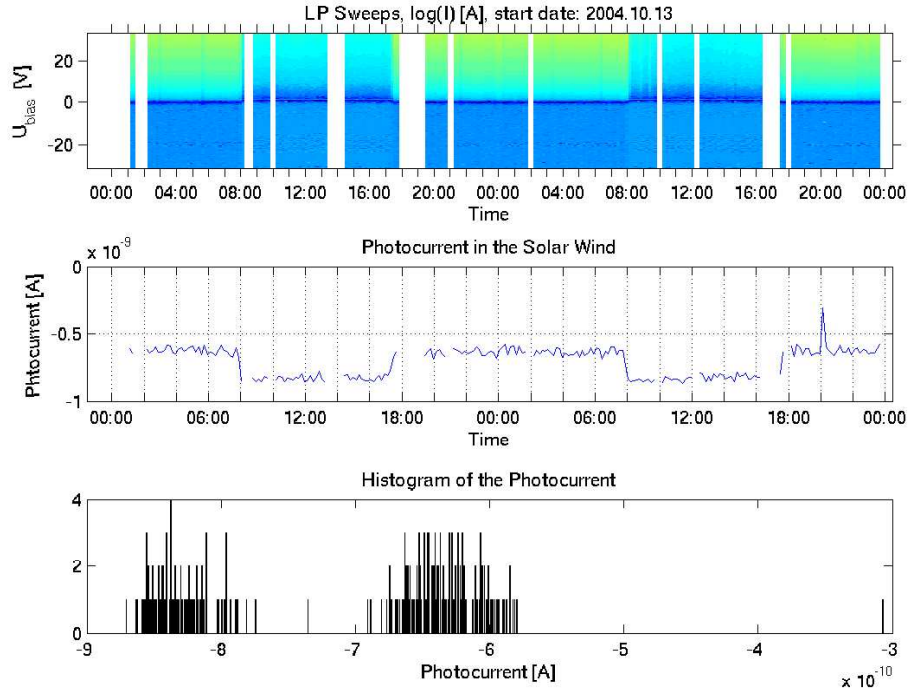


Figure 11.1: Cassini in the solar wind

11.2 Inside the magnetopause

The characteristics for the magnetosphere are the more changing values. It is still possible to see the alternating colours in the very highest part of the positive part of the sweep (upper plot in Fig. 11.4). The photocurrent is continuously jumping between two levels (middle plot in Fig. 11.4). When the histogram of the photocurrent is analysed two peaks appear. When comparing the bias jump of the photocurrent and the changes in the sweep, conclusion to be made is that they occur at the same time (Fig. 11.4). When the histogram (Fig. 11.5) of the entire period is analyzed (when the satellite is in the magnetosphere), three peaks can be seen. Peak one and two are not that well separated. When comparing this histogram with the histogram of the short interval (lower plot in Fig. 11.4). Peak one and two can be identified, while peak three seem not to be found. The two peaks are not well separated because the values are changing more when the spacecraft

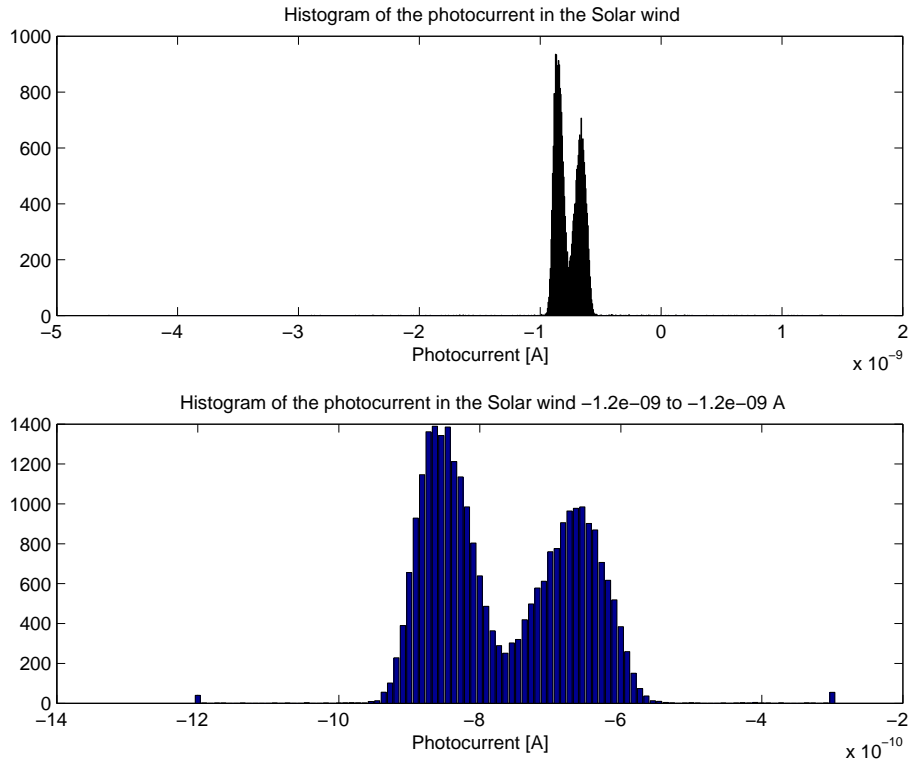


Figure 11.2: Histogram of the probe current in the Solar Wind

is inside the magnetosphere compared to the more stable values measured in the solar wind. The conclusion that the bias jump is an ongoing process within the magnetopause still holds. The best explanation for the third peak is that it belongs to data collected in low-density plasma. Table 11.2 shows the time when Cassini is in high density plasma.

11.3 Close flybys and the perigee of Saturn

When looking at the close flybys of any of the moons and the perigee of Saturn the data changes rapidly and go to different extreme values. This can be seen in the two upper plots in figure 11.6 which shows the perigee of Saturn. The lower plot shows the histogram and the data is widely spread. This data would not represent the solar intensity because the density in the plasma is too high and the probe measures some other processes than the intended. These sections may be viewed as unwanted data

Table 11.1: When Cassini is in the solar wind

From	To
-	29/6 -04 00:00
5/7 -04 00:00	26/10 -04 12:00
5/11 -04 00:00	13/12 -04 10:00
22/12 -04 00:00	14/1 -05 00:00
23/1 -05 04:00	13/2 -05 12:00
24/2 -05 08:00	28/2 -05 24:00

Table 11.2: When Cassini is in high density plasma

From	Distance, R_s	To	Distance, R_s
29/6 -04 00:00	31	5/7 -04 00:00	37
26/10 -04 12:00	20	5/11 -04 00:00	42
13/12 -04 10:00	20	22/12 -04 00:00	42
14/1 -05 00:00	20	23/1 -05 04:00	42
13/2 -05 12:00	30	24/2 -05 08:00	42

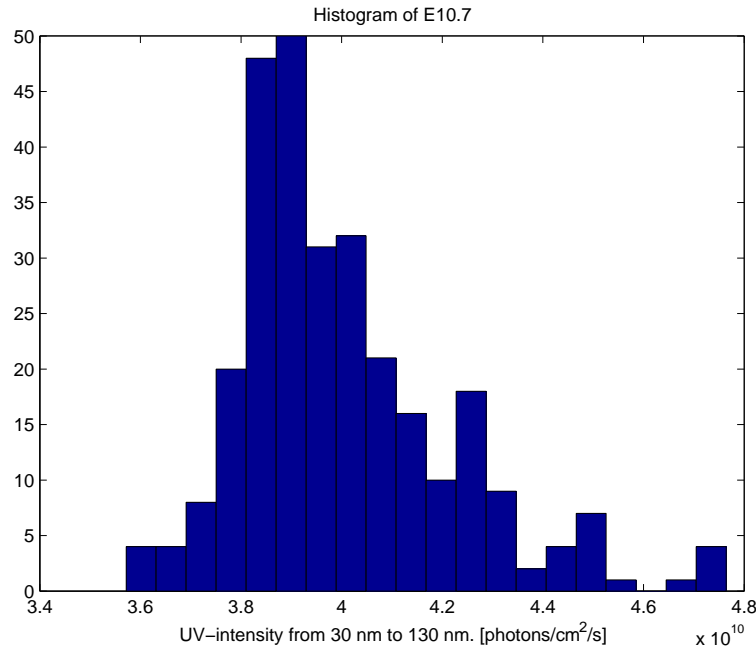


Figure 11.3: Histogram E10.7

and be excluded when estimating the solar intensity. Table 11.3 shows the dates when flybys and the Saturn perigee are performed.

11.4 The bias jump

The photocurrent makes a bias jump in both the solar wind and in the magnetosphere, but the E10.7 is a continuous process. The conclusion is that some other process also is measured in addition to the solar intensity. Because the photocurrent is making a bias jump at the same time as there is a change in the positive range of the sweep the conclusion is that they are caused by the same phenomena. The bias jump seem to affect the photocurrent in the same way as in sampled square-wave would do. The bias jump only changes the value with a constant value, so the signal from the probe can be described as:

$$S_{probe} = s_{photocurrent} + a \times s_{square-wave} \quad (11.1)$$

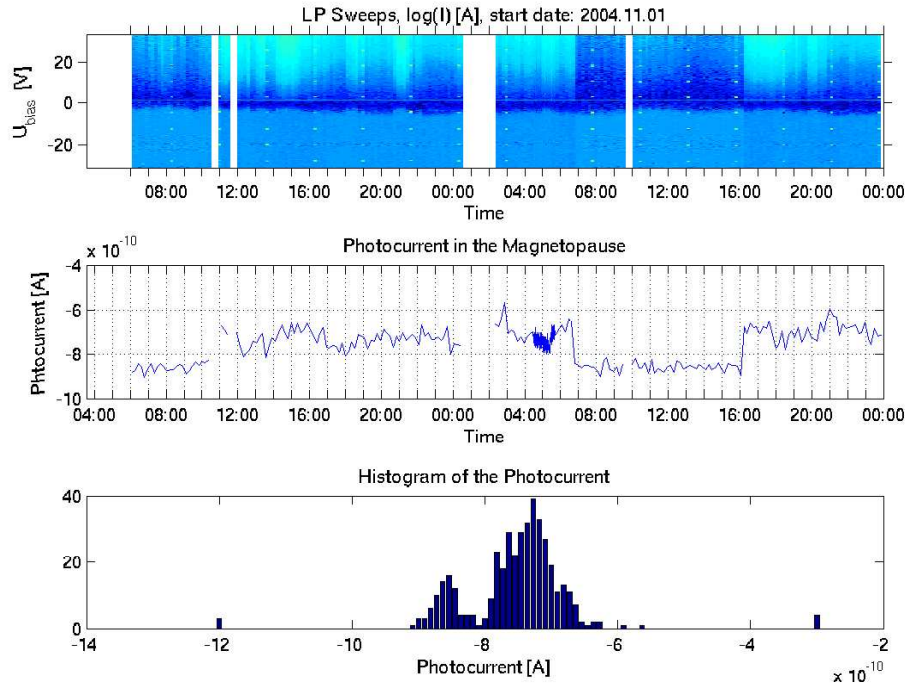


Figure 11.4: Cassini in the high density plasma

11.5 The channels that measure the photocurrent

The channels that measure the photocurrent have a mean value that is dependent on the electrical potential. The more negative the channel is, the stronger the measured photocurrent be, even if the measurement is made at the same time. The variance and the mean value of the signal is shown for the solar wind and the magnetosphere in figure 11.5 and figure 11.8. The change of variance and mean value of each channel is shown for the sweeps from 0 to -32 V. When the two figures are compared it is possible to draw the conclusion that the same channels can be used for both the solar wind and the magnetosphere when measuring the photocurrent. When measuring the UV-intensity, all the channels should measure the same process and the changes in the UV-intensity is slow. Those channels that shows a large change in mean value or variance compared to the surrounding channels can be excluded because they are probably measuring some other process than the photocurrent. In figure 11.5 and figure 11.8 it is possible to see that a few channels separates widely from the others. The chosen interval of the probe sweep for

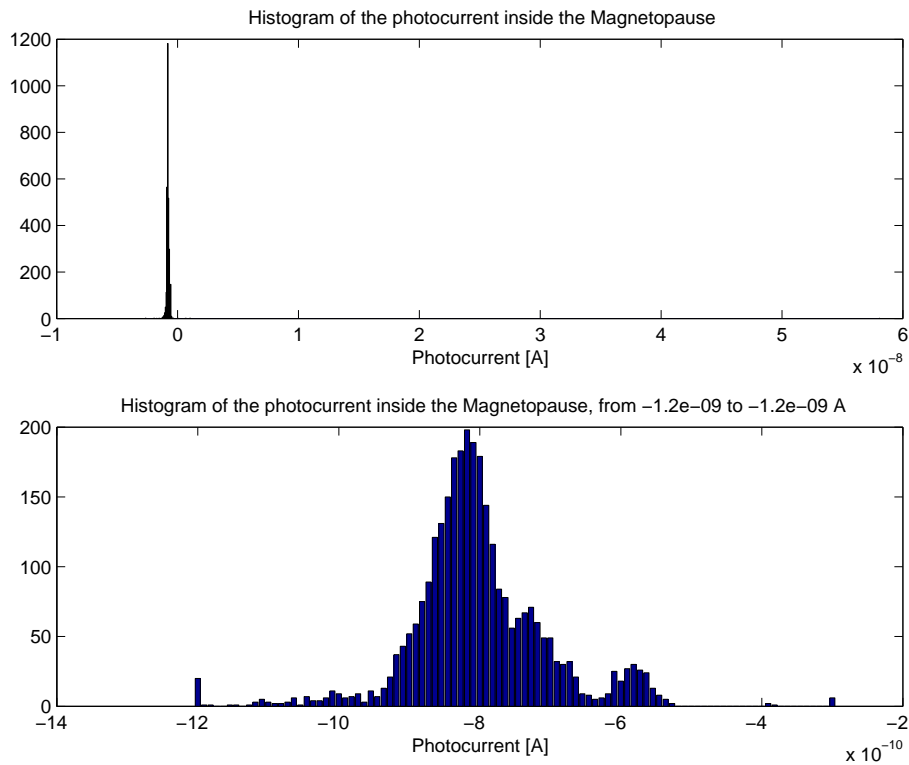


Figure 11.5: Histogram of the probe current in high density plasma

calculating the photocurrent is shown in Table 11.4.

11.6 Noise reduction

The resolution of 10 minutes is much higher than needed for measuring the UV-intensity. The highest resolution needed for this purpose would be something around 6-12 hours because of the slow changes in the solar intensity. This reduction of the sample frequency may reduce the noise and there are several methods that can do this operation.

Table 11.3: When Cassini is doing a close flyby

Object	From	Distance, R_s	To	Distance, R_s
Saturn	1/7 -04 00:00	5	1/7 -04 12:00	7
Titan	26/10 -04 12:00		26/10 -04 13:00	
Saturn	28/10 -04 00:00	7	29/10 -04 06:00	10
Titan	13/12 -04 10:00		13/12 -04 14:00	
Saturn	14/12 -04 10:00	10	15/12 -04 22:00	10
Titan	14/1 -05 12:00		14/1 -05 18:00	
Saturn	16/1 -05 06:00	5	16/1 -05 24:00	10
Saturn	16/2 -05 12:00	9	17/2 -05 14:00	9

Table 11.4: The selected intervals of the potential sweep

From, V	To, V
-6	-7.4
-8	-9.25
-9.75	-10.4
-11.4	-13.1
-14.3	-16
-20	-22.7
-22.8	-27.6

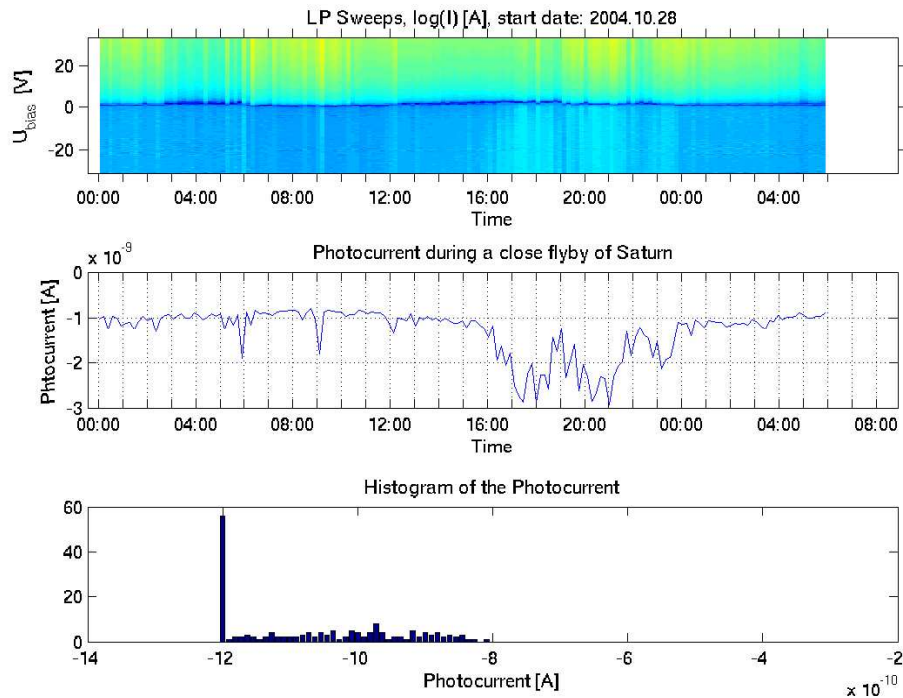


Figure 11.6: The Saturn Flyby at the 29th of October 2004

11.7 Improvement of signal

To improve the signal, there are different methods that may be applied to remove the various distortions, enhance the wanted signal and the measurement of the photocurrent. This sort of data analysis is a subjective way of evaluating the dataset. There is no exact science determining which method to use and where the limit should be drawn between a wanted and an unwanted value. The result from the data quality analysis shows that there is a bias jump that greatly changes the measured signal. The bias jump is on the same magnitude as the yearly changes of E10.7, see figure 11.3. For that reason it is necessary to remove the bias jump to enhance the quality of the photocurrent. This distortion is most likely safe to remove because the solar intensity does not make this abrupt jump, on the contrary, it is continuous in its change. Also there are no indications that this would be anything else than an instrumental effect. There are no predictions that the plasma around Saturn would have this characteristic.

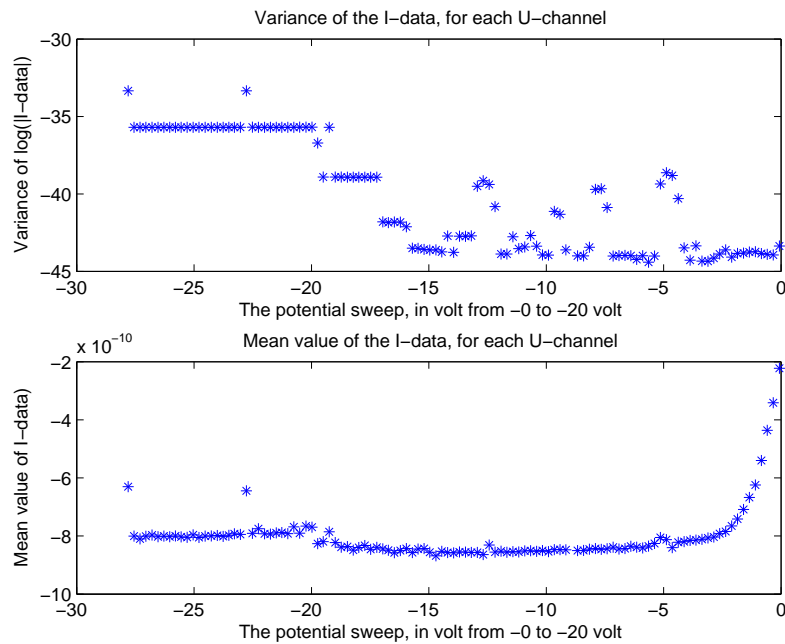


Figure 11.7: The mean value and the variance of the potential sweep in the solar wind

11.8 Identification of Outliers

Outliers are extreme data points that most likely do not belong to the dataset of the measured photocurrent. The physical reasons for these outliers might be a local higher density in the plasma on crossing the magnetopause or just prior to or following a close flyby. These extreme values greatly affect the calculations of the UV-intensity because they might be 1000 times larger than the other values. Outliers can be detected by the following two methods. Both of these methods need to be treated with caution as there is no dependency in time and the wanted signal is indeed time dependent.

11.8.1 A global lower and higher cut off value

The outliers are identified by looking at the histogram for the entire dataset to find a suitable higher- and lower cut off value. This makes it possible to classify all values as outliers or non-outliers. It is necessary that the histogram of the signal

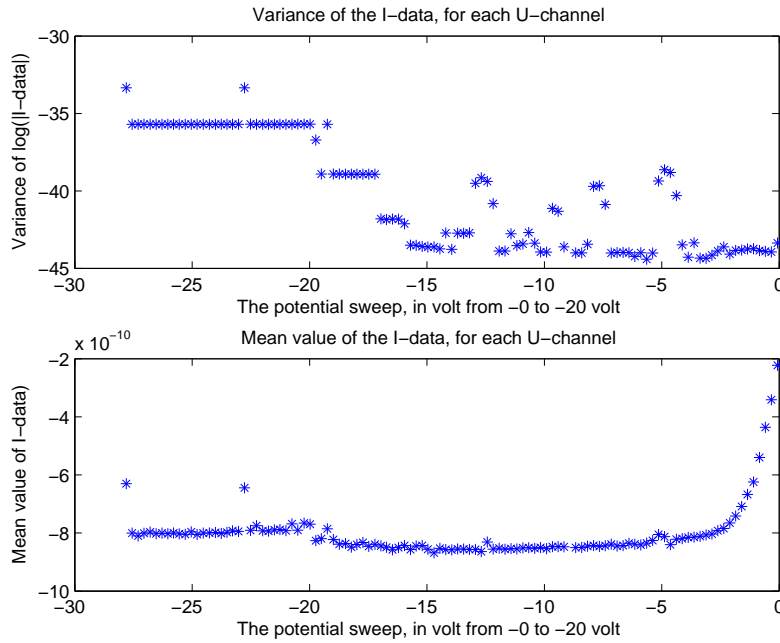


Figure 11.8: The mean value and the variance of the potential sweep in the magnetopause

get updated with time, to make sure the entire part of the signal is included. In figure 11.9 all of the data from the photocurrent i is shown. The data outside the selected interval will be treated as outliers.

11.8.2 A local cut off value, based on a estimation of a normal distribution

As all data, I are divided into subsets I_{subset} where each subset contains data from the period:

$$I_{subset} = I(t_0) \rightarrow I(t_0 + dt) \quad (11.2)$$

where dt is the length of the time interval.

Within this subset the signal is assumed to be stationary and if the subset contains enough data points, it may be assumed to form a normal distribution [9]. The mean value and the variance of this distribution can be estimated. The probability for

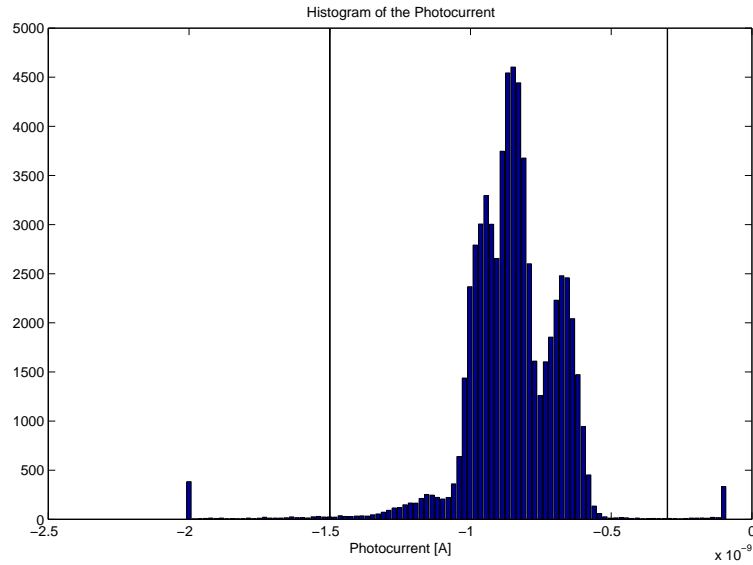


Figure 11.9: The distribution of the photocurrent

each point i_t to belong to this distribution can be estimated by using the formula [9]:

$$P_{i_t} \in N(m, \sigma) \quad (11.3)$$

where i_t is the probe current at time t .

Again a cut off values is estimated. The length of the time interval, which creates the subsets, is important because local time independents are assumed. If the length of the time interval gets too long, local changes might disappear. If the subset does not contain enough data points the approximation to a normal distribution cannot be made.

11.9 Removal of the square wave

Assuming there are two signals measured s_1 and s_2 and the two signals are representing s_{photo} and s_{square} form the Langmuir probe. Because the height of the square wave almost has the same height as the yearly changes of E10.7, it is necessary to remove that signal from the photo current. The signal can be divided into

two sub signals, the signal at the two levels of the square wave. The main goal is to separate the two signals, make a bias adjustment, so that the two signals turn into one signal.

11.10 Separating the two signals

There is a large difference between the potential sweep for the solar wind, where the density is low, and during the close passage of Saturn, when the density is high. This divides the classification into two different cases: one for the solar wind and one for the magnetosphere. This creates the need for a classification process, which can handle when the satellite is in both the solar wind and in the magnetosphere. The current is linear related to the potential when the sweep is collected [?], thus a rather small interval of 1 volt is suitable when selecting the classification interval.

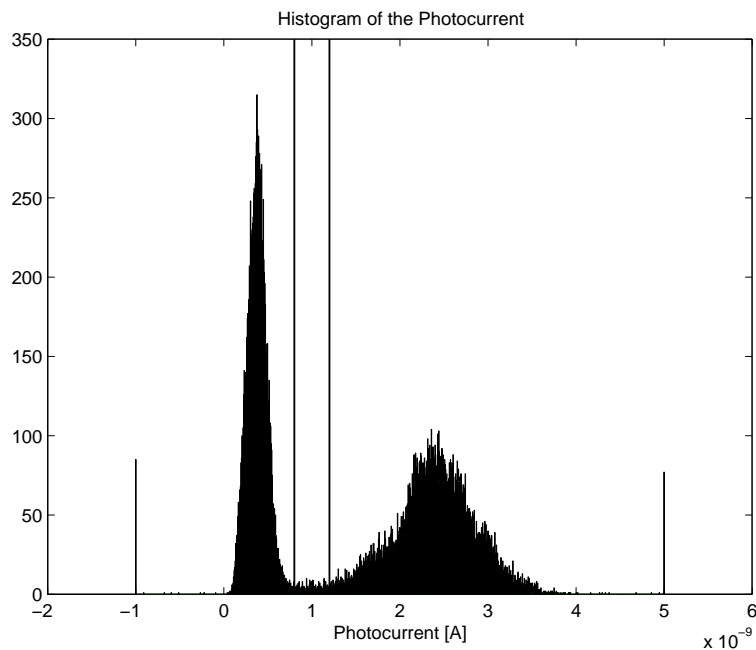


Figure 11.10: The distribution of the photocurrent

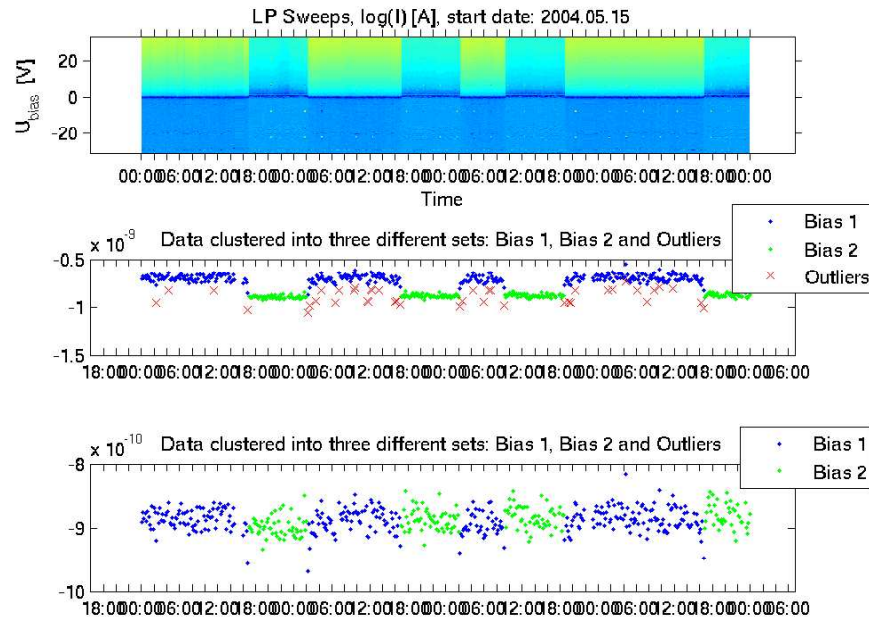


Figure 11.11: Data classified in the solar wind

11.11 Classification criteria for the solar wind

When looking at the histograms of the photocurrent, the two signals are represented by two clear peaks (Fig. 11.2). When looking on the positive side, the two signals are clearly separated with a very distinct boundary (Fig. 11.10). The difference in intensity between the two peaks and the gap in between is at a ratio 1000:1, which means very few wrong classifications. The points in the gap, may be classified as uncertain, and the later be classified depending on the classification of the surrounding points. The histogram of the photocurrent when the satellite is in the solar wind provides decision criteria, because the peaks are well separated at 2 – 3 volt. (Fig. 11.10). Values above $1.2 \times 10^{-9}A$ are classified as signal 1. Values below $0.8 \times 10^{-9}A$ are classified as signal 2. Values between $0.8 \times 10^{-9}A$ and $0.8 \times 10^{-9}A$ are not classified. In Fig. 11.10 the two peaks are shown and between the two peaks there is a region which is difficult to classify. Fig. 11.11 show an example of the classification result.

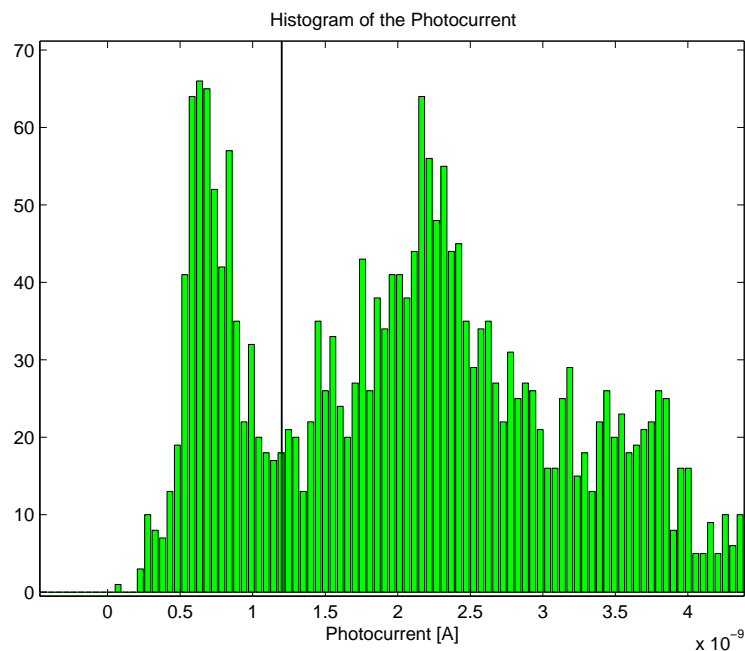


Figure 11.12: The distribution of the photocurrent

11.12 Classification criteria for the magnetopause

When looking for a separator in the high density area, it is not as clearly visible as in the solar wind. If the current is analysed, there is a clear bias jump and the same conclusion may be made from the twin peaks in the histogram (Fig. 11.5). At the higher density area, the peaks are well separated at 20 – 21 volt (Fig. 11.12). Values below $0.8 \times 10^{-9}A$ are classified as signal 2. The two peaks are shown, but there is no real gap between the two peaks. Figure 11.13 show an example of the classification result.

11.13 Unclassified points

The unclassified points will be classified by a most likely method based on the photocurrent from signal 1 and signal 2. Both the signals will be approximated as a normal distribution. The probability for the unclassified points to belong to one of the distributions will be calculated. Then the unclassified points can be classified

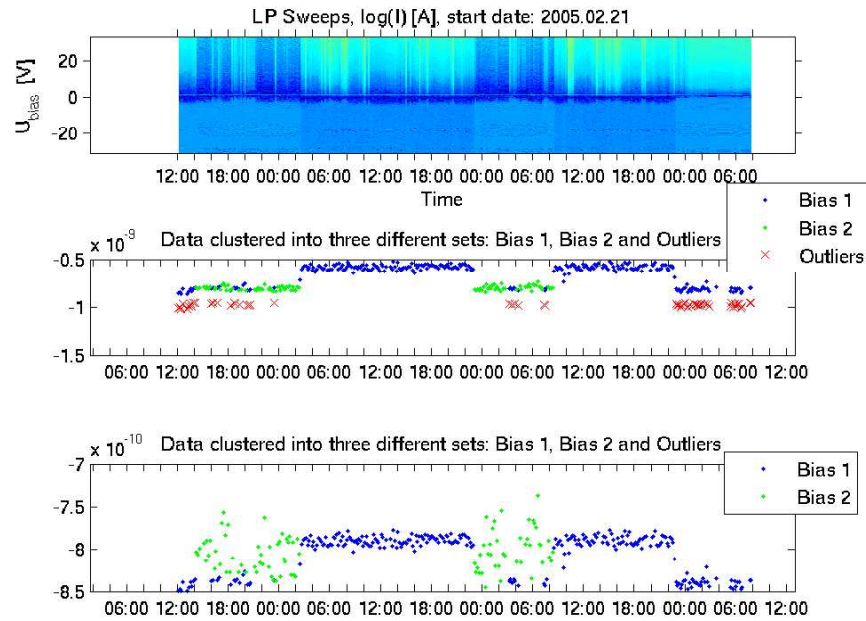


Figure 11.13: Data classified in the MP

to the most likely signal.

11.14 Evaluation of the classifiers

Both classifiers create a very good result when classifying within the designated area: within the solarwind and within the magnetosphere. Figure 11.11 and figure 11.13 shows example of the result of the classification. However both classifiers will classify almost all points to the same signal when the data from the opposite section is classified. Figure 11.14 and figure 11.15 shows the result of the classification when the wrong classifier is used.

11.15 Which separator to use

The selection of which separator to be used will be based on their performance. Both classifiers will be used at the same time on each subset. The classifier that provides the best result will be used on that subset. The level of success will be

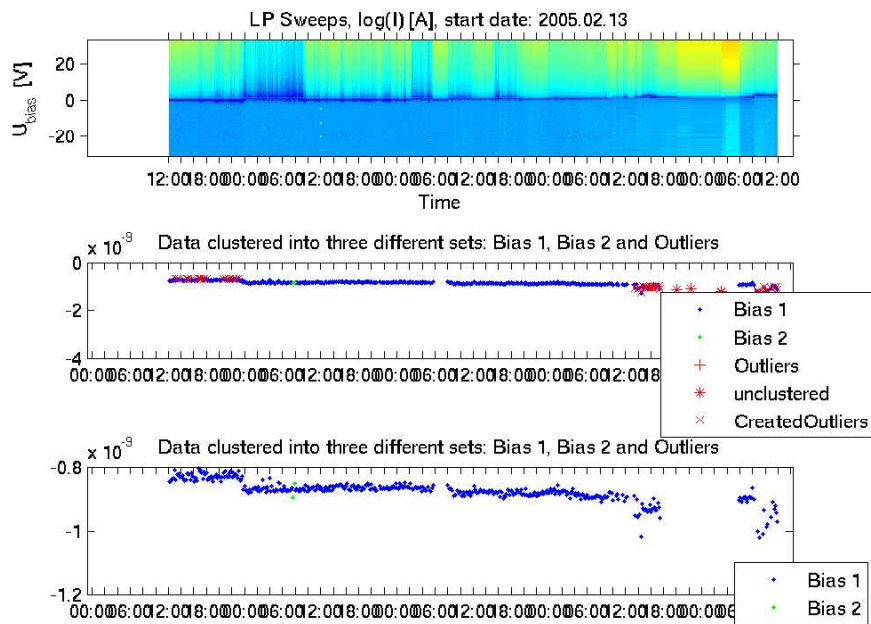


Figure 11.14: MP data classified with the Solar wind

measured through observing the decrease in the variance of the signal. This gives an upper limit of the length of the window used for adjusting the signal, as the section when the satellite is closest to Saturn are one to four days. If the window is too long, data may be classified to the wrong signal if the subset contains both solar wind and magnetosphere data.

11.16 Selecting a reference signal

The better of the two signals is the one corresponding to the higher and narrower peak. This signal has less background noise in comparison with other one. For that reason it is selected as the reference signal. When looking at the two signals, signal one follows E10.7 much better in amplitude, but is very noisy. Signal two follows the trends in E10.7 better and the signal contains less noise.

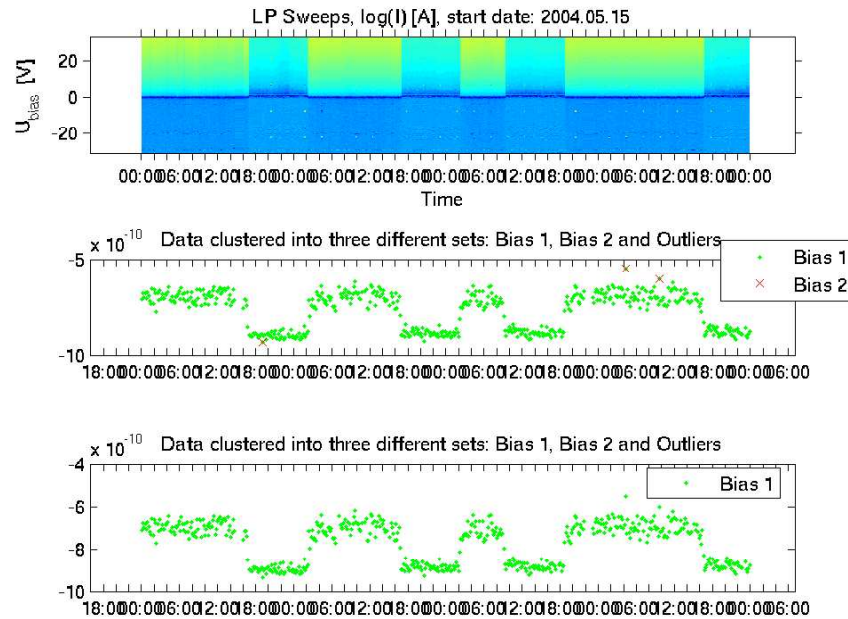


Figure 11.15: Solar wind data classified with the MP-classifier

11.17 Merging the two signals

After assigning one of the signal as the reference signal, the other signal can be normalised and then converted back, but now with the mean-value and the variance of the reference signal. The two signals are now merged and can be treated as one. The noise of the second signal is reduced to the same level as the reference signal. This method may create a few exceptions that will need to be handled.

- If there is no reference signal for a time interval, the previous time interval will be used.
- If there is no variance for one of the signals, the variance one will be used, meaning there will only be a change in bias.
- If the reference signal has a higher variance than the other signal, a variance of one will be used again. Otherwise more noise will be brought into the signal.

11.18 Algorithm for improving the signal

1. All unwanted date periods are excluded.
2. A timeline for the time interval is created, starting from the first date and then with a length of a specified number of days.
3. All the data belonging to that interval is selected.
4. All data points with a NaN sweep will be removed.
5. Each data point above the upper or below the lower cut off limit (in the interval of the photocurrent) will be classified as an outlier.
6. The entire signal is normal approximated and outliers are removed according to a cut-off value.
7. The following steps are made using two different methods: One when in the solar wind, and the other for within the magnetosphere.
8. Each data point is classified regarding to the positive classification potential as either:
 - Reference signal.
 - Not reference signal.
 - Uncertain, between the reference and the other signal in the histogram, above the lower classification limit and below the upper classification limit.
9. The uncertain data points are classed as the more probable of the two signals, regarding to the normal approximation of the photocurrent.
10. The two methods and the original signal are compared and the one with the smallest variance is selected as the best classifier.
11. The two signals are merged.
12. A new normal approximation is made to remove all potentially created outliers and normal outliers, according to a cut-off value.

Chapter 12

Result

12.1 Result from test 1

The expected result was achieved.

12.2 Result from test 2

The test displays good accuracy, especially as Earth and Venus line up against the Sun (Nov. 1981 to Feb. 1982 in Fig. 12.1). Both the trends and the bias level fit between PVO-data and E10.7. The analytical value of c is 1.53×10^{11} and the statistically value of c is 2.43×10^{11} , which has to be seen as a good accuracy, because both the methods are independent from each other. Fig. 12.1 shows the the E10.7 value and the estimated value of the UV-intensity between 1981 to 1984. The estimated value is calculated by using the Langmuir probe data from PVO. Both the long term and the short term trends match and the accuracy improves as the common solar disc seen from Earth and Venus get larger. The level of the UV-intensity between the reference and the estimated intensity are also well aligned.

12.3 Results from test 3 - without data adjustment

Fig. 12.2 shows the estimated UV-intensity for different time resolutions; 12 hours, 24 hours and 48 hours. The method gives a good result for the period August 2004 to January 2005 if an averaging period of 48 hours is used. There is a good agreement between the reference data and the estimated UV-intensity. Solar trends are visible and the bias level is accurate. After January 2005 the method can not give any reliable result, because the time the spacecraft spends in the solar wind has decreased as the orbit time has gone shorter.

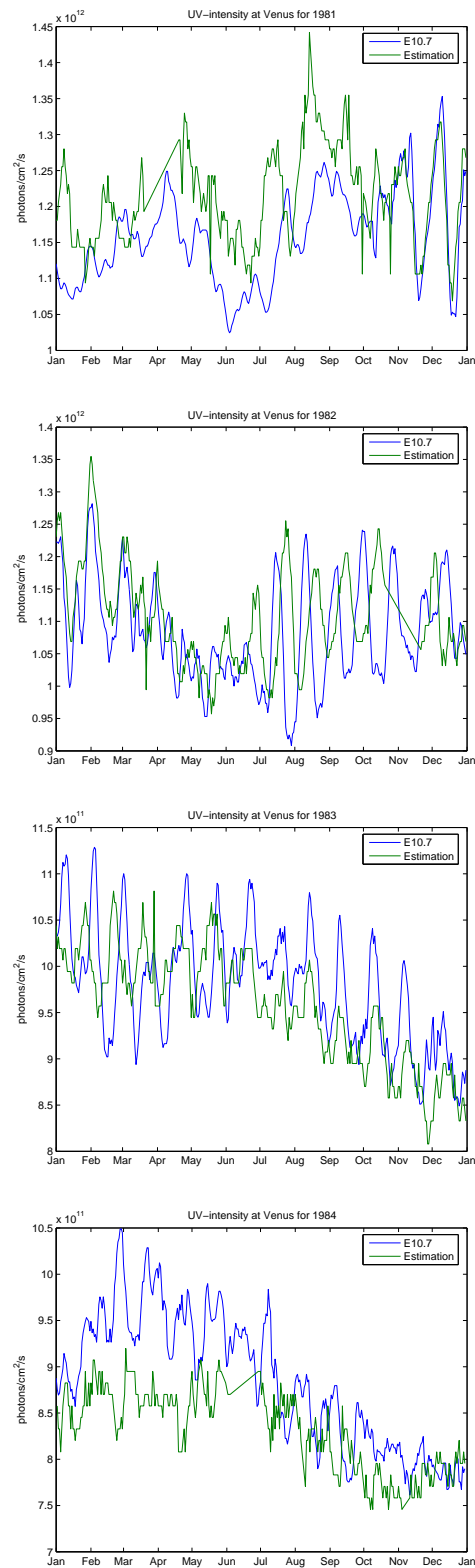


Figure 12.1: $E_{10.7}$ and estimated UV-intensity at Venus made by PVO from 1981 to 1984

Interesting result:

- When Cassini travels through high density plasma a clear signature from the Langmuir probe, which would make it possible to auto detect a flyby.

12.4 Results from test 3 - with data adjustment

Figure 12.3 and figure 12.4 shows the result of the UV-estimation when using S_1 , S_2 and S_{1and2} . When only using S_1 , the worst result is obtained. When using S_{1and2} with a bias adjustment the best result is obtained. The conclusion from this is that it is worth the effort to adjust the data by removing the difference in the bias level between S_1 and S_2 , instead of only using one of the signals.

Fig. 12.4 shows the estimated UV-intensity for different time resolutions; 12 hours, 24 hours and 48 hours. For the time-period June 2004 to January 2005, when most of the time is spent in the solar wind, the adjustment for the data works well. It is possible to run with a time resolution of 12 hours and the method gives a good result. The estimated UV-intensity is aligning well with E10.7 when viewing the bias level and the trends.

After January 2005 the accuracy in the result decreases as Cassini spends less time in the solar wind. If a time resolution of 24 hours is selected the result seem to be good. The data adjustment works well, but false peak might be introduced when the satellite is in high density plasma. The best way to remove this source of error is to exclude these periods.

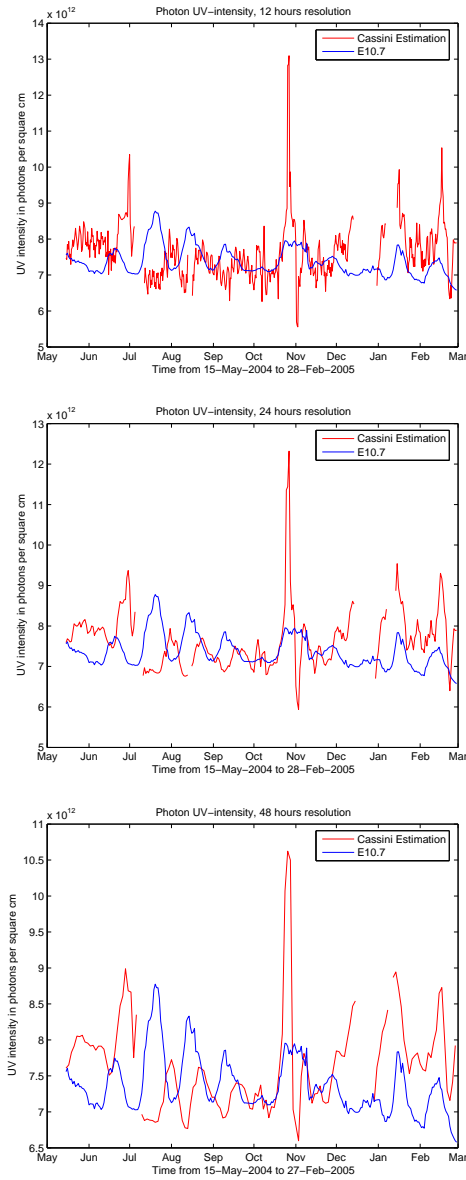


Figure 12.2: Estimated UV-intensity in the solar wind at Saturn made by Cassini, without data adjustment

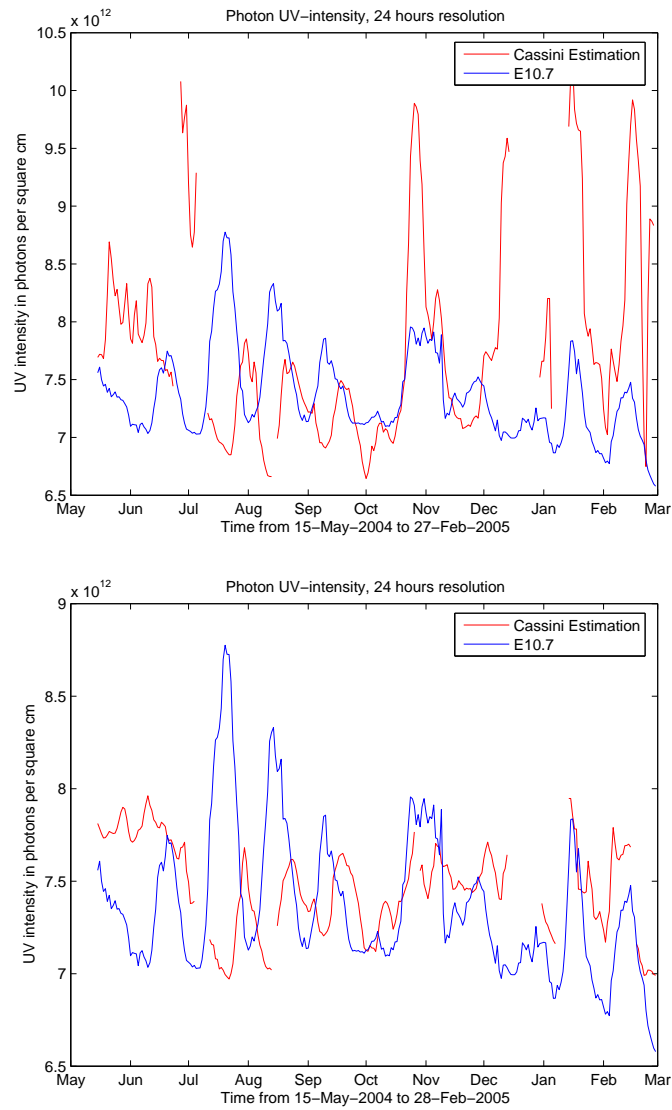


Figure 12.3: Estimated UV-intensity at Saturn made by Cassini, with signal S_1 and S_2 , 24 hours resolution

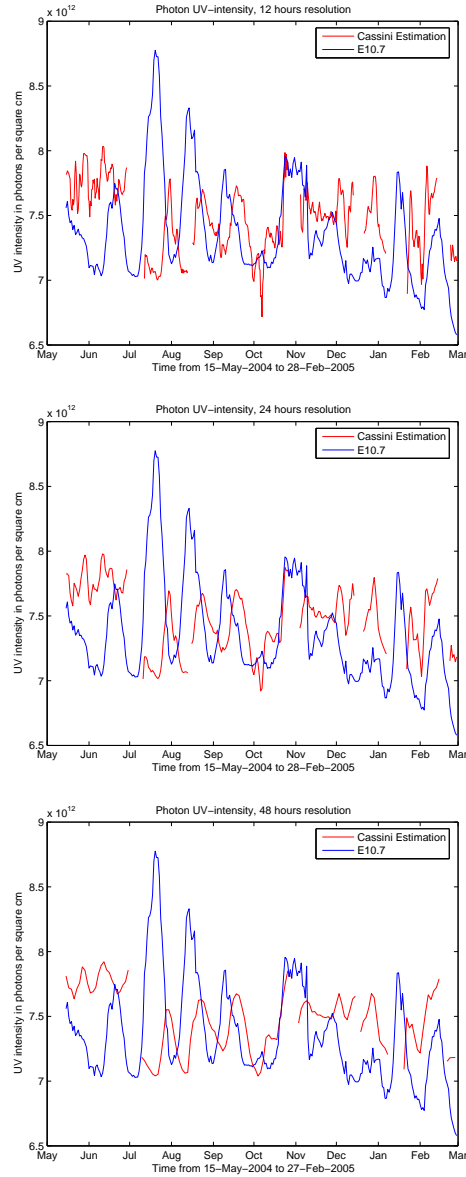


Figure 12.4: Estimated UV-intensity at Saturn made by Cassini, with data adjustment

Chapter 13

Conclusions and Discussion

13.1 Conclusion of test results

The statistical method provides good results when tested on the Venus Pioneer-data and the difference between the statistical value and their analytical value is 50%. The test on Cassini is not as successful, but the results are still acceptable. When Cassini is orbiting with the furthest point 6 times the size of the magnetopause the result is good, the noise in the data is low, the trends and the intensity level agrees well with the reference data. When Cassini flies in the smallest orbit, with the furthest distance twice the size of the estimated magnetopause, the noisy signal increases the needed length of the averaging window. At the same time the orbit time reduces by half, 15 days. This makes it difficult to see the long-term solar trends and to compare it with E10.7 after the 15th of January 2005. This is not a malfunction of the method, but a result from a systematic error causing a bias jump. When the signal is filtered a good result is given before the 15th of January and reasonable result is given after that date.

13.2 Conclusion of the data analysis

It appears that the signal from the photocurrent is sampled together with a square-wave, which has a large effect on the noise of the signal. The size of this square wave seem to be depending on the distance of the satellite to the magnetopause.

13.3 Discussion about the cause of the square wave

The square signal may have three different causes; A physical reason, a transmission error, or a handling error. The physical reason can be divided into to different

reason, a real phenomena, which is correctly measured or a physical phenomena caused by the satellite interacting with the surrounding environment. The noise may also be a man made error caused by mishandling of the data. This is the reason why the cause of the phenomena should be investigated further. The effect of the phenomena can be seen in the Cassini RPWS LP Sweep, where there is a drastic change in the area 0-32 volt; these changes are connected in time when the square wave makes the bias jump. Potential causes could be:

- Another instrument affecting the environment.
- The satellite changing its orientation in space, which could change its electrical potential.
- Error in interpreting the collected data.
- Badly performed calibration.
- Badly handled data.

Without a proper investigation being done it seems like the bias jump is caused by the attitude of the satellite. This change or the spacecrafts orientation in space it made to point a camera in the right direction.

Acknowledgments

Bibliography

- [1] D.L. Krichnet D.A. Gurnett, W.S. Kurth. The cassini radio and plasma wave investigation. *Space Science Reviews*, 114:396–463, 2004.
- [2] A. Einstein. *Ann. d. Phys.*, (20):199, 1906.
- [3] W. K. Tobiska et al. The solar2000 empirical solar irradiance model and forecast tool. *Journal of Atmospheric and Solar-Terrestrial Physics*, 62:1233–1250, 2004.
- [4] Space Environment Technologies. <http://www.spacewx.com/solar2000.html>.
- [5] D. T. Russel M. G. Kivelson. *Introduction to Space Physics*. The Press Syndicate of the University of Cambridge, 1995.
- [6] Planet's Orbits. <http://www.alcyone.de/>.
- [7] R.F. Theis L. H. Brace, W.R. Hoegy. Solar euv measurements at venus based on photoelectron emission from the pioneer venus langmuir probe. *Journal of Geophysical Research*, 93(A7):7282–7296, 1988.
- [8] I. Langmir Mott-Schmitt. *Phys. Rev.*, 28(272):7282–7296, 1926.
- [9] G. Blom. *Sannolihetsteori med tillämpningar*. Studentlitteratur, andra edition, 1984.
- [10] A. Tjulin R. Behlke, D. Sundkvist. Langmuir probes contributed chapter in sensors and instruments for space exploration. 2000.